A Simulation Technique For Multi-Variate Non-Gaussian Stochastic Fields

Fumio Yamazaki
University of Tokyo, Tokyo, Japan
Masanobu Shinozuka
Princeton University, Princeton, NJ USA

ABSTRACT

A digital generation method for multi-variate multi-dimensional non-Gaussian homogeneous stochastic fields is proposed. The method first generates Gaussian sample fields based on spectral representation and then maps them into non-Gaussian sample fields with the aid of an iterative procedure. A numerical example indicates that this algorithm works well and generated sample fields satisfy the target spectral density functions and the probability distribution functions in ensemble sense. The proposed method is considered to have a wide range of applicability to engineering problems involving multi-variate multi-dimensional stochastic fields where the Gaussian assumption is not appropriate

INTRODUCTION

The methods of digitally generating sample functions of stationary and nonstationary stochastic processes have been well established in the last two decades or so on the basis of the spectral or AR/ARMA representation techniques. The same observation can be made for the methods of generating sample functions of homogeneous or nonhomogeneous stochastic fields. These models have been extensively used in various applications in the areas of engineering mechanics and structural engineering. More recently, the problems of system stochasticity have attracted considerable attention and interest among engineers and researchers. In this respect, the theory of stochastic fields has been advanced (e.g., Vanmarcke, 1983; Shinozuka, 1987) and the methods of digitally generating sample functions for the purpose of Monte Carlo solution of finite element analysis problems involving stochastic fields have been developed (e.g., Yamazaki, Shinozuka and Dasgupta, 1987).

However, because of mathematical difficulties and the lack of observed data, most generation techniques as well as analytical approaches are limited to dealing with Gaussian fields. In some situation, such a Gaussian assumption is not appropriate because the observed fields exhibit non-Gaussian characteristics. For example, even if the input motions are Gaussian, the output responses of nonlinear systems are known to be non-Gaussian. Also, strictly speaking, the spatial variability of Young's modulus and some other material properties should not be considered to form Gaussian fields since they are not supposed to take negative values. Thus the development of a method for generating sample functions of non-Gaussian fields appears to have theoretical as well as practical significance.

As one of the few studies in this direction involving non-Gaussian processes, Shinozuka and Tan (1981) demonstrated such a generation method in which the prescribed crossing rate is reproduced by mapping a Gaussian process into a non-Gaussian process while at the same time reproducing the prescribed irregularity ratio in approximation. A more general generation method has recently developed for non-Gaussian multi-dimensional homogeneous fields by Yamazaki and Shinozuka (1988). The method utilizes an iterative procedure involving the generation method for Gaussian homogeneous fields on the basis of their spectral representation, and the mapping technique which transforms Gaussian sample functions into non-Gaussian sample functions. In this paper, this technique is further extended to dealing with multi-variate multi-dimensional non-Gaussian stochastic fields.

SIMULATION OF MULTI-VARIATE MULTI-DIMENSIONAL GAUSSIAN STOCHASTIC FIELDS

The digital generation method for Gaussian multi-variate multi-dimensional stochastic fields is described in detail herein in order to facilitate the introduction of simulation and generation methods for non-Gaussian fields. A general procedure for generation of nD-mV (n-dimensional and m-variate) stochastic fields have been developed by Shinozuka and Jan (1972) and modified by Shinozuka (1987).

Consider a set of m homogeneous Gaussian n-dimensional stochastic fields $f^0_j(\mathbf{x})$ $(j=1, 2, \cdots, m)$ with mean zero: $E[f^0_j(\mathbf{x})]=0$ in an n-dimensional space $\mathbf{x}=[x_1\ x_2 \cdots x_n]^T$. The auto-correlation function $R^0_{jk}(\boldsymbol{\xi})$ $(j=k)$ and the cross-correlation function $R^0_{jk}(\boldsymbol{\xi})$ $(j\neq k)$ are defined by $R^0_{jk}(\boldsymbol{\xi})=E[f^0_j(\mathbf{x}_r)f^0_k(\mathbf{x}_s)]$ with $\boldsymbol{\xi}=\mathbf{x}_r-\mathbf{x}_s$ being the separation vector. Assuming that an n-fold Fourier transform of $R^0_{jk}(\boldsymbol{\xi})$ exists, the power $(j=k)$ or cross $(j\neq k)$ spectral density function of $f^0_j(\mathbf{x})$ is defined by the n-dimensional version of the Wiener-Khintchine transform pair. Then the cross-spectral density matrix $\mathbf{S}^0(\boldsymbol{\kappa})$ is constructed:

$$\mathbf{S}^0(\boldsymbol{\kappa}) = \begin{bmatrix} S^0_{11}(\boldsymbol{\kappa}) & S^0_{12}(\boldsymbol{\kappa}) & \cdots\cdots & S^0_{1m}(\boldsymbol{\kappa}) \\ S^0_{21}(\boldsymbol{\kappa}) & S^0_{22}(\boldsymbol{\kappa}) & \cdots\cdots & S^0_{2m}(\boldsymbol{\kappa}) \\ \cdots\cdots & \cdots\cdots & \cdots\cdots & \cdots\cdots \\ S^0_{m1}(\boldsymbol{\kappa}) & S^0_{m2}(\boldsymbol{\kappa}) & \cdots\cdots & S^0_{mm}(\boldsymbol{\kappa}) \end{bmatrix} \tag{1}$$

with $\boldsymbol{\kappa}=[\kappa_1\ \kappa_2 \cdots \kappa_n]^T$ indicating the wave number vector.

Suppose now one can find a matrix $\mathbf{H}(\boldsymbol{\kappa})$ which possesses an n-dimensional Fourier transform and satisfies the equation:

$$\mathbf{S}^0(\boldsymbol{\kappa}) = \mathbf{H}(\boldsymbol{\kappa})[\overline{\mathbf{H}}(\boldsymbol{\kappa})]^T \tag{2}$$

with the super bar indicates the complex conjugate. To find $\mathbf{H}(\boldsymbol{\kappa})$ in an efficient way, we assume that $\mathbf{H}(\boldsymbol{\kappa})$ is a lower triangular matrix. Then the solutions are obtained (Shinozuka and Jan, 1972).

Once $\mathbf{H}(\boldsymbol{\kappa})$ is computed, the field $f_j(\mathbf{x})$ can be simulated in an efficient way by the following series:

$$f_j(\mathbf{x}) = \sqrt{2}\sum_{m=1}^{j}\ \sum_{l_1=-N_1}^{N_1}\ \sum_{l_2=-N_2}^{N_2} \cdots \sum_{l_n=-N_n}^{N_n} |H_{jm}(\kappa_{1l_1}, \kappa_{2l_2}, \cdots, \kappa_{nl_n})| \sqrt{\Delta\kappa_1 \Delta\kappa_2 \cdots \Delta\kappa_n}$$

$$\cdot \cos\left(\kappa_{1l_1}x_1 + \kappa_{2l_2}x_2 + \cdots + \kappa_{nl_n}x_n + \theta_{jm}(\kappa_{1l_1}, \kappa_{2l_2}, \cdots, \kappa_{nl_n}) + \phi_{m l_1 l_2 \cdots l_n}\right) \tag{3}$$

where $\phi_{ml_1l_2\cdots l_n}$ is an independent random phase angle uniformly distributed between 0 and 2π, and the spectral density function $S^0_{jk}(\boldsymbol{\kappa})$ is considered to be of insignificant magnitude outside the region defined by $-\boldsymbol{\kappa}_u \leqq \boldsymbol{\kappa} \leqq \boldsymbol{\kappa}_u$. Also each interval is $\Delta\kappa_i=\kappa_{iu}/N_i$ and the wave number vector is

$$\boldsymbol{\kappa}_l = [\kappa_{1l_1}\ \kappa_{2l_2} \cdots \kappa_{nl_n}]^T \ ; \quad \kappa_{il_i} = l_i\,\Delta\kappa_i \ ; \quad l_i = 1, 2, \cdots, N_i \ ; \quad i=1, 2, \cdots, n \tag{4}$$

and the argument of the polar form representation of $H_{jm}(\boldsymbol{\kappa}_l)$

$$\theta_{jm}(\kappa_{1l_1}, \kappa_{2l_2}, \cdots, \kappa_{nl_n}) = \tan^{-1}\left[\frac{\operatorname{Im} H_{jm}(\kappa_{1l_1}, \kappa_{2l_2}, \cdots, \kappa_{nl_n})}{\operatorname{Re} H_{jm}(\kappa_{1l_1}, \kappa_{2l_2}, \cdots, \kappa_{nl_n})}\right] \tag{5}$$

If $N_1, N_2, \cdots, N_n \rightarrow \infty$ simultaneously, the simulated field $f_j(\mathbf{x})$ is asymptotically Gaussian by virtue of the central limit theorem. It can be shown that the expected value and correlation functions of the simulated field are the same as the target ones in ensemble sense, i.e., $E[f_j(\mathbf{x})]=E[f^0_j(\mathbf{x})]=0$ and $R_{jk}(\boldsymbol{\xi})=R^0_{jk}(\boldsymbol{\xi})$; $j, k=1, 2, \cdots, m$. Also, it can be shown that the simulated field is ergodic at least to be second moment. The Fast Fourier transform (FFT) algorithm can be introduced in Eq. 3 under the assumption that the stochastic field possesses zero power at the origin $\mathbf{S}^0(0)$ and quadrant symmetry.

EVALUATION OF SPECTRAL DENSITY FROM SAMPLE FIELDS

The method of evaluating the spectral density functions from a sample field is described. For a sample function $f^{(s)}_j(\mathbf{x})$ defined in the range $0\leqq x_i \leqq L_i$ $(i=1, 2, \cdots, n)$, the n-fold Fourier transform is obtained by

$$F^{(s)}_j(\boldsymbol{\kappa}) = \int_0^{L_n} \cdots \int_0^{L_2}\int_0^{L_1} f^{(s)}_j(\mathbf{x})\, e^{-i\boldsymbol{\kappa}\cdot\mathbf{x}}\, dx_1 dx_2 \cdots dx_n \tag{6}$$

where $\boldsymbol{\kappa}\cdot\mathbf{x}$ is the inner product of $\boldsymbol{\kappa}$ and $\mathbf{x}$. Note $L_i=M_i\Delta\xi_i=2\pi/\Delta\kappa_i$. The sample cross-spectral density function is, then, defined for this finite region by

$$S_{jk}^{(s)}(\kappa) = \frac{1}{(2\pi)^n L_1 L_2 \cdots L_n} \overline{F}_j^{(s)}(\kappa) F_k^{(s)}(\kappa) \tag{7}$$

The spatial cross-spectral density function can be obtained as the limit of Eq. 7:

$$<S_{jk}^{(s)}(\kappa)> = \lim_{L_1, L_2, \cdots, L_n \to \infty} \frac{1}{(2\pi)^n L_1 L_2 \cdots L_n} \overline{F}_j^{(s)}(\kappa) F_k^{(s)}(\kappa) \tag{8}$$

Also, the ensemble cross-spectral density function is

$$S_{jk}(\kappa) = E\left[\frac{1}{(2\pi)^n L_1 L_2 \cdots L_n} \overline{F}_j^{(s)}(\kappa) F_k^{(s)}(\kappa) \right] \tag{9}$$

This ensemble cross-spectral density function can be estimated by the Monte Carlo method by

$$S_{jk}(\kappa) \approx \frac{1}{N_s} \sum_{s=1}^{N_s} S_{jk}^{(s)}(\kappa) \tag{10}$$

for the sample size N_s. The spectral density functions defined by Eqs. 8 and 9 satisfy their target:

$$<S_{jk}^{(s)}(\kappa)> = S_{jk}(\kappa) = S_{jk}^{0}(\kappa) \tag{11}$$

If the FFT algorithm is taken advantage of, however, Eq. 8 is difficult to obtain because huge memory space and CPU time are required when $L_i \to \infty$. Hence Eq. 10 (as an approximate form of Eq. 9) is utilized in a numerical example of this study. Note that for uni-variate stochastic fields, the sample spectral density function (Eq. 7) exactly satisfies its target for periods L_i. For multi-variate stochastic fields, however, such a convenient relationship is no more valid except for the sub-field 1 ($j=1$ in Eq. 3).

DIGITAL GENERATION OF MULTI-VARIATE MULTI-DIMENSIONAL NON-GAUSSIAN STOCHASTIC FIELDS

A method for digitally generating sample functions of multi-variate multi-dimensional non-Gaussian homogeneous stochastic fields is developed. This method is an extended version for multi-dimensional non-Gaussian homogeneous stochastic fields (Yamazaki and Shinozuka, 1988). The flow chart of the method is shown in Fig. 1.

First, the target spectral density matrix $\mathbf{S}_{bb}^{(T)}(\kappa)$ (T indicates the target) and the one-dimensional (marginal) probability distribution function $F_{B_j}(b_j)$ of the multi-variate ($j=1, 2, \cdots, m$) non-Gaussian stochastic field are specified. Here b_j denotes the j-th non-Gaussian stochastic field (of a multi-variate stochastic field) with zero mean and variance $\sigma_{b_j}^2$. Correspondingly, one can easily find the Gaussian probability distribution function $F_{G_j}(g_j)$ with zero mean and variance $\sigma_{g_j}^2 = \sigma_{b_j}^2$.

The first step of the method is to assume the power ($j=k$) and cross ($j \neq k$) spectral density functions of the Gaussian field to be $\mathbf{S}_{g_jg_j}^{(1)}(\kappa) = \mathbf{S}_{b_jb_j}^{(T)}(\kappa)$, and generate a sample function of the Gaussian field $g_j^{(1)}(\mathbf{x})$ by Eq. 3. Then the simulated field $g_j^{(1)}(\mathbf{x})$ is transformed into the non-Gaussian field $b_j^{(1)}(\mathbf{x})$ by a mapping technique; or generally the simulated field $g_j^{(i)}(\mathbf{x})$ of the i-th iteration is mapped into $b_j^{(i)}(\mathbf{x})$ at $\mathbf{x}_p$ ($p=1, 2, \cdots, M_1 M_2 \cdots M_n$) as

$$b_j^{(i)}(\mathbf{x}_p) = F_{B_j}^{-1}[F_{G_j}(g_j^{(i)}(\mathbf{x}_p))] \tag{12}$$

on each probability distribution function diagram. If the number of data points is large enough, Eq. 12 generates the sample field with the target non-Gaussian distribution function. However, the sample power or cross-spectral density $S_{b_jb_k}^{(i)}(\kappa)$ calculated by Eq. 7 does not coincide with the target spectral density $S_{b_jb_k}^{(T)}(\kappa)$. This reason is two fold; one is the transformation represented by Eq. 12 is nonlinear, and another is the sample spectral density cannot satisfy its target within a finite period of space as mentioned previously. In order to overcome the first problem, an iterative algorithm is introduced. The spectral density for generating the Gaussian stochastic field in the $(i+1)$ iteration is assumed as

$$S_{g_jg_k}^{(i+1)}(\kappa) = \frac{\hat{S}_{g_jg_k}^{(i)}(\kappa)}{\hat{S}_{b_jb_k}^{(i)}(\kappa)} S_{b_jb_k}^{(T)}(\kappa) \tag{13}$$

where the hat indicates the smoothed power and cross-spectral density functions after applying a spectral window in wave number domain. For this purpose, a multi-dimensional version of the Hanning window (e.g., Bendat and Piersol, 1971) is employed. Note that for cross-spectral density functions, this smoothing

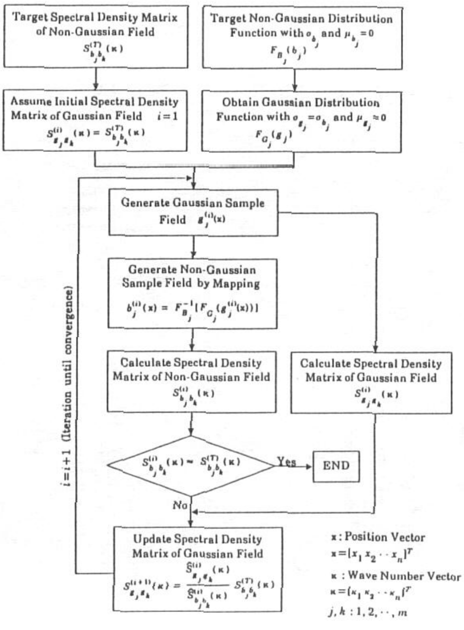

Fig. 1 Flow Chart for Generation of Non-Gaussian Multi-Variate Stochastic Fields

is carried out for the real and imaginary parts independently. The reason why such a spectral window technique is introduced is to obtain numerical stability in the following iterative scheme to realize the target cross-spectral density matrix. For uni-variate cases, however, such numerical stability can be obtained without recourse to the spectral window technique (Yamazaki and Shinozuka, 1988).

Following the same procedure as used in the first iteration, the Gaussian field of the i-th iteration, $g_j^{(i)}(\mathbf{x})$, is generated using the updated $S_{g_j g_k}{}^{(i)}(\kappa)$ and the same random phase angles. Updating the spectral density for the Gaussian field in terms of Eq. 13 is performed for the following reasons. Through the nonlinear mapping represented by Eq. 12, the spectral density for each wave number changes. However, the rate of change at each wave number which is represented by the ratio $S_{g_j g_k}{}^{(i)}(\kappa)/S_{b_j b_k}{}^{(i)}(\kappa)$ may be expected to approach a constant value in a few iterations. Unfortunately, however, this supposition is found to be not so correct for multi-variate cases as for the uni-variate cases. Hence, in order to force $S_{b_j b_k}{}^{(i+1)}(\kappa)$ to approach $S_{b_j b_k}{}^{(T)}(\kappa)$ as i increases, Eq. 13 is devised. This iterative algorithm has been proven to work efficiently in the following numerical example.

NUMERICAL EXAMPLE

A bi-variate two-dimensional non-Gaussian homogeneous field is considered as an example of general multi-variate multi-dimensional fields. As a typical example of a non-Gaussian distribution, the beta distribution is assumed which has the following probability density function:

$$f_B(b) = \frac{1}{B(q,r)} \frac{(b-b_{min})^{q-1}(b_{max}-b)^{r-1}}{(b_{max}-b_{min})^{q+r-1}} \qquad (b_{min} \leqq b \leqq b_{max}) \tag{14}$$

in which b_{min} and b_{max} are the lower and upper bounds of the distribution, q and r are parameters of the distribution, and $B(q, r)$ is the beta function. The shape of the density function can be controlled by choosing appropriate values for q and r. For a bi-variate stochastic field, two different distributions are considered by assuming $q_1=4$ and $r_1=2$ for field 1 (the first sub-field), and $q_2=2$ and $r_2=2$ for field 2 (the second sub-field). Also, $\mu_b=\mu_{b_1}=\mu_{b_2}=0$ and $\sigma_b=\sigma_{b_1}=\sigma_{b_2}=1.0$ are assumed. The probability density functions and probability distribution functions of these beta distributions are shown in Fig. 2 along with those of the Gaussian distribution of zero mean and unit standard deviation.

The following cross-spectral density matrix is assumed as the target without loss of generality.

$$\mathbf{S}^{(T)}(\kappa) = \begin{bmatrix} S_{11}^{(T)}(\kappa) & S_{12}^{(T)}(\kappa) \\ S_{21}^{(T)}(\kappa) & S_{22}^{(T)}(\kappa) \end{bmatrix} = \begin{bmatrix} 1 & \beta^* \\ \beta & 1 \end{bmatrix} \times \sigma_b^2 \frac{d^2}{4\pi} \exp\left[-\left(\frac{d\,|\kappa|}{2} \right)^2 \right] \tag{15}$$

in which d is a parameter representing the decay of the correlation, β indicates the complex constant representing cross-correlation, and the asterisk is the complex conjugate. The value of β is taken as $\beta=\beta^*=0.7$ which represents strong positive correlation between fields 1 and 2. Note that when the phase delay of the two fields is considered, β becomes a complex number. For this cross-spectral density matrix, the corresponding lower triangular matrix $\mathbf{H}(\kappa)$ is obtained as follows:

$$\mathbf{H}(\kappa) = \begin{bmatrix} \sqrt{S_{11}^{(T)}(\kappa)} & 0 \\ \dfrac{S_{21}^{(T)}(\kappa)}{\sqrt{S_{11}^{(T)}(\kappa)}} & \dfrac{\sqrt{S_{11}^{(T)}(\kappa)S_{22}^{(T)}(\kappa) - |S_{21}^{(T)}(\kappa)|^2}}{\sqrt{S_{11}^{(T)}(\kappa)}} \end{bmatrix} \tag{16}$$

The target spectral density functions are shown in Fig. 3 with constants $d=1.0$, $\kappa_{1u}=\kappa_{2u}=1.6\pi$, and $N_1=N_2=32$. The Gaussian stochastic field is generated by Eq. 3 with the number of data points equal to 4096 ($M_1=M_2=64$). By following the mapping and iterative procedure, the bi-variate non-Gaussian stochastic field following the beta distributions is generated after 3 iterations and shown in Fig. 4. The generated Gaussian and beta fields are compared along the line $y=0$ in Fig. 5 in which the effect of nonlinear mapping can be observed.

By using the different sets of random phase angles in Eq. 3, one hundred bi-variate Gaussian and non-Gaussian sample stochastic fields are generated, and the ensemble spectral density functions thus obtained are depicted in Fig. 6. This figure clearly indicates that the generated stochastic fields satisfy their targets in ensemble sense. A better agreement may be obtained for a larger sample size. Considering the ergodicity of the generated fields, the statistical distributions of the 4,096 data points in a sample field are plotted in Fig. 7 with their analytical forms. It is observed that the beta distributions are generated with high accuracy. Therefore, the simulated sample field is proved to satisfy both the target cross-spectral density matrix and probability distribution functions. The proposed generation method may be applied to any forms of the distribution function and the cross-spectral density matrix. A further study is required, however, to demonstrate wide applicability of the method.

CONCLUSION

A method of digitally generating sample functions of multi-variate multi-dimensional non-Gaussian homogeneous stochastic fields is proposed as an extended version of the method for multi-dimensional non-Gaussian homogeneous stochastic fields developed by the present authors. First, the target power and cross-spectral density functions and the target probability distribution functions of the zero-mean multi-variate non-Gaussian field are specified. Then, a corresponding multi-variate Gaussian stochastic field having the same means and variances is defined. Sample functions of the Gaussian field are generated so as to reproduce the target spectral density functions of the non-Gaussian field. These sample functions are transformed into the sample functions of the non-Gaussian field by mapping on the probability distribution function diagrams. Through the mapping operation, the means and variances are unchanged. However, the spectral density functions of the resulting non-Gaussian field will be different from the target, since the operation is nonlinear. Then, the spectral density functions of the Gaussian field is updated so that the sample function of the non-Gaussian field obtained by the mapping satisfies the target spectral density functions. A spectral window technique is employed in this process for the stability of sample spectral density functions. In a few iterations of the updating of the spectral density functions and the mapping operation, the generated non-Gaussian field satisfies the target spectral density functions in ensemble sense. Also the target probability distribution function is satisfied.

A numerical example is demonstrated for a bi-variate two-dimensional stochastic field whose one-dimensional distribution functions are two different beta distributions. After three iterations, the sample function closely reproduced the prescribed beta distributions and spectral density functions. It is noted that the proposed method can be applied to multi-variate multi-dimensional stochastic fields with any (one-dimensional) distribution forms. Therefore the method may be an extremely useful tool for generating sample functions of homogeneous but non-Gaussian fields.

ACKNOWLEDGMENT

In performing this work, F. Yamazaki was supported by Ohsaki Research Institute, Shimizu Corporation, Japan and M. Shinozuka by NSF Grant No. MSM-83-18123, USA.

REFERENCES

Bendat, J. S., and Piersol, A. G. (1971). *Random Data: Analysis and Measurement Procedures*, John Wieley & Sons, Inc., New York, NY.

Shinozuka, M. (1987). "Stochastic Fields and Their Digital Simulation," *Stochastic Methods in Structural Dynamics*, edited by G. I. Schuëller and M. Shinozuka, M. Nijhoff Publishers, Netherlands, pp. 93-133.

Shinozuka, M., and Jan, C-M. (1972). "Digital Simulation of Random Processes and Its Applications," *Journal of Sound and Vibration*, Vol. 25, No. 1, pp. 111-128.

Shinozuka, M., and Tan, R.Y. (1981). "Probabilistic Load Combinations and Crossing Rates," *Proc. of the symposium on Probabilistic Methods in Structural Engineering*, ASCE, pp. 229-250.

Vanmarcke, E. (1983). *Random Fields*, MIT Press, Cambridge, MA.

Yamazaki, F., and Shinozuka, M. (1988). "Digital Generation of Non-Gaussian Stochastic Fields," *Journal of Engineering Mechanics*, ASCE, Vol. 114, No. 7, pp. 1183-1197.

Yamazaki, F., and Shinozuka, M., and Dasgupta, G. (1988). "Neumann Expansion for Stochastic Finite Element Analysis," *Journal of Engineering Mechanics*, ASCE, Vol. 114, No. 8, pp. 1335-1354.

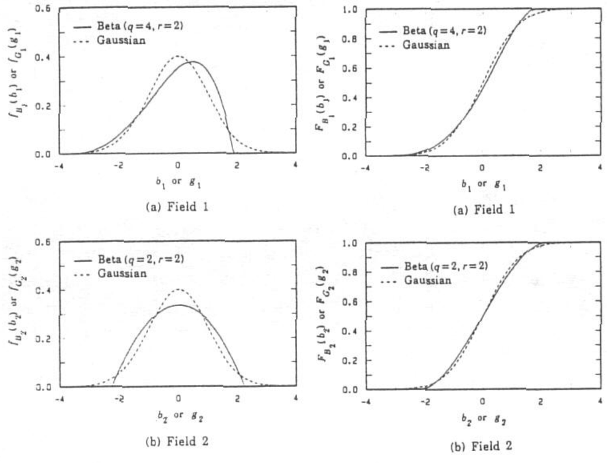

Fig. 2 Target Probability Density Functions and Probability Distribution Functions

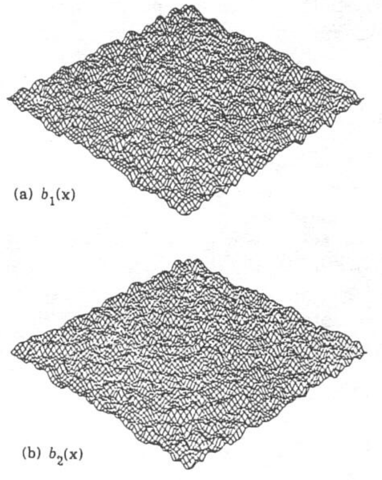

Fig. 4 Simulated Bi-Variate Beta Stochastic Field

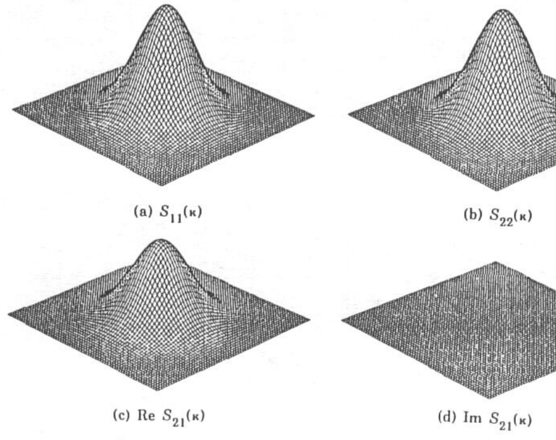

Fig. 3 Target Spectral Density Functions

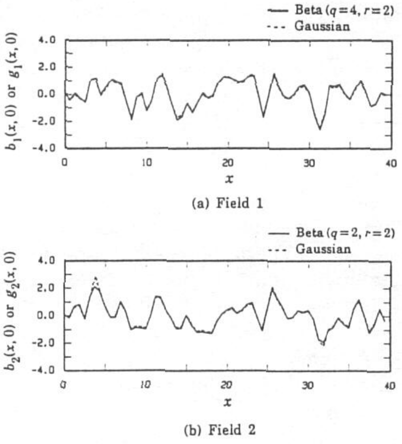

Fig. 5 Simulated Stochastic Fields along $y=0$

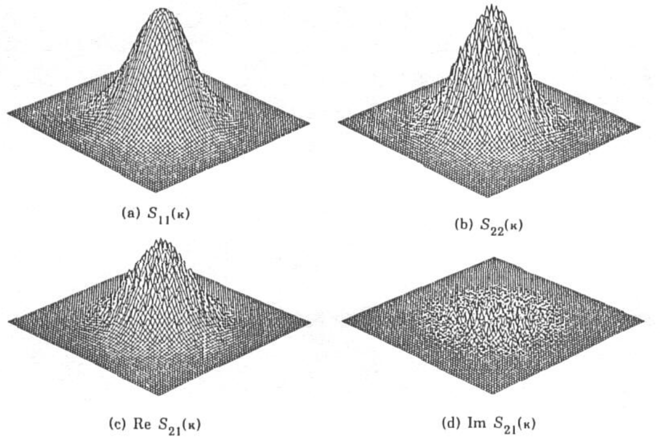

Fig. 6 Ensemble Spectral Density Functions

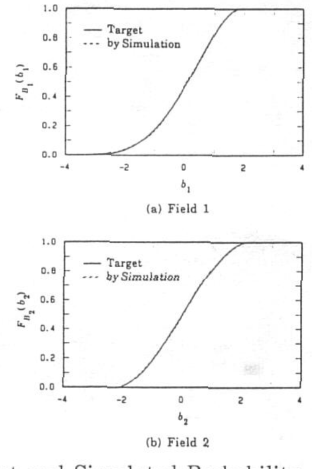

Fig. 7 Target and Simulated Probability Distribution Functions of Beta Field